



## Detecting land degradation in Southern Africa using Time Series Segment and Residual Trend (TSS-RESTREND)

Zidong Li<sup>a</sup>, Shuai Wang<sup>a,\*</sup>, Shuang Song<sup>a</sup>, Yaping Wang<sup>a</sup>, Walter Musakwa<sup>b</sup>

<sup>a</sup> State Key Laboratory of Earth Surface Processes and Resource Ecology, Faculty of Geographical Science, Beijing Normal University, Beijing, 100875, PR China

<sup>b</sup> Department of Town and Regional Planning, Faculty of Engineering and The Built Environment, University of Johannesburg, Johannesburg, South Africa



### ARTICLE INFO

**Keywords:**

Southern Africa  
Land degradation  
Precipitation-vegetation relationship  
Breakpoint  
TSS-RESTREND

### ABSTRACT

Land degradation is a universal environmental problem around the world, which affects 1.5 billion people's well-being. Therefore, the efforts to monitor where land degradation has happened and to find out the causes are meaningful for land management and restoration. Arid regions such as Southern Africa have attracted many concerns on land degradation assessment. However, previous studies have neglected the impacts of rainfall variation and possible breakpoints. In this study, the Time Series Segment and Residual Trend (TSS-RESTREND) method was used to detect land degradation in southern Africa and to compare with linear regression, RESTREND methods. Using TSS-RESTREND, 73.22% of the study area was found with vegetation controlled by precipitation, and 18.9% of the study area was found with breakpoints detected. Besides, results demonstrated that these increasing, decreasing, unchanged, and indeterminate pixels respectively made up 21.32%, 9.67%, 42.23%, and 26.78% of the study area. By eliminating positive effects from precipitation and including negative effects from breakpoints, TSS-RESTREND highlighted the potential overestimate of improvement by the linear regression method and the underestimate of degradation by the linear regression and RESTREND methods. These results showed that the land degradation detection with TSS-RESTREND method is useful for land conservation and restoration.

### 1. Introduction

Land degradation is a universal environmental problem around the world (Spinoni et al., 2015) and usually reduces the capability of the land to provide ecosystem goods and perform functions and services that support society and development (Hassan, 2005). Global land degradation assessment indicated that 24% of the global land area with degrading existing, which areas are home to 1.5 billion people (Bai et al., 2008). Therefore, efforts to monitor where land degradation has happened and to find out the causes are meaningful for land management and restoration. With remote-sensing techniques, most studies use the normalized difference vegetation index (NDVI) as a proxy for vegetation productivity to detect long-term declines in ecosystem productivity by linear regression analysis and the nonparametric MK test (Higginbottom and Symeonakis, 2014). As a result of climatic variations and human activities (UNCED, 1994), land degradation is related to extreme precipitation and temperature (Kalisa et al., 2019), soil moisture (Wei et al., 2019), cropland extension (Matlhodi et al., 2019), and

deforestation (Silva et al., 2019).

Southern Africa includes ten countries in the southern part of Africa, which is composed of more than 70% arid land and is home to 105.6 million people (Cervigni, R., & Morris, 2016). Given the high vulnerability of vegetation to environmental dynamics and disturbances, Southern Africa has attracted many concerns on land degradation detection and assessment on regional and local scales (Bai et al., 2008; Klintenberg and Seely, 2004). However, different indicators used and unmatched period make the results of these studies incomparable, which failed to reveal the extent and intensity of degradation in Southern Africa. For example, the results from degradation risk assessment in Namibia calculated with grazing density and population (Klintenberg and Seely, 2004) are not comparable for land degradation assessment in South Africa with data of forage productivity (Wessels et al., 2004). Moreover, results calculated with data from 1971 to 1999 (Klintenberg and Seely, 2004) are also not comparable with data from 1951 to 2010 (Spinoni et al., 2015). Therefore, to provide more evidence-based information for land-use management and sustainable development, a

\* Corresponding author. State Key Laboratory of Earth Surface Processes and Resource Ecology Faculty of Geographical Beijing Normal University, Beijing, 100875, PR China.

E-mail address: [shuawaiwang@bnu.edu.cn](mailto:shuawaiwang@bnu.edu.cn) (S. Wang).

degradation assessment including all countries of Southern Africa and with the same indicators is needed.

In arid regions, vegetation dynamics are mainly controlled by rainfall (Helldén and Tottrup, 2008). In such cases, changes in vegetation index caused by increasing precipitation may mask degradation (Wessels et al., 2012). Consequently, the Residual Trend (RESTREND) analysis was proposed and applied to detect land degradation with rainfall impacts eliminated (Bai et al., 2008; Wessels et al., 2012). Under the assumption of a significant correlation between precipitation and vegetation ( $P < 0.05$ ), the residual of precipitation-vegetation relationship was regressed over time (Wessels et al., 2012). With the RESTREND method, degradation induced by human activities had been detected in China (Xue et al., 2019) and a positive residual trend was determined to be related to shrub encroachment (Saha et al., 2015). Besides, given ongoing climatic change and intensified human activities, the vegetation-precipitation relationship (VPR) is likely to have changed. For example, a breakpoint in VPR that presents structural change may emerge after extreme drought. And it will breakdown the assumption of the RSETREND method (Smith et al., 2019). Consequently, the time-series segment and residual trend analysis (TSS-RESTREND) was put out to incorporate the influence from breakpoints into RESTREND, with breakpoints detected by Breaks for Additive Seasonal and Trend (BFAST) and Chow test (Burrell et al., 2017). Using the TSS-RESTREND method, Burrell et al. (2017) has detected breakpoints induced by bushfires and the decline of rabbit overgrazing in Australia and corrected the underestimate of degradation by RESTREND. Similarly, Southern Africa is mainly made up of arid land, and the strong relationship between vegetation and precipitation has been proved (Sedano et al., 2016). Under the dynamics of climate (Spinoni et al., 2015) and human activities, the ecosystem composition and the residual trends have probably changed. However, previous studies have neglected the impacts of rainfall variation and possible breakpoints. Consequently, this study aim to apply TSS-RESTREND to detect land degradation in Southern Africa and to compare the performance of linear regression, RESTREND, and TSS-RESTREND techniques. Finally, the drivers of degradation were also analyzed to provide a qualitative evaluation of the performance of TSS-RESTREND.

## 2. Study area

The study area is composed of ten countries in Southern Africa (Angola, Zambia, Zimbabwe, Malawi, Mozambique, Namibia,

Botswana, South Africa, Lesotho, and the Republic of Eswatini). Aridity Index is defined as  $P$  (Precipitation)/ETP (potential evapotranspiration) (FAO, 2016). In Southern Africa, the most of study area is composed of arid land with aridity index  $<0.65$ , and from the northeast to the southwest, the aridity index decrease, which means the increasing stress from aridity (Zomer et al., 2008). Besides, Southern Africa has a wide diversity of land cover, including tree cover, shrub cover, herbaceous cover, and bare cover, besides these there are land covers controlled by human being like cropland and artificial land (Fig. 1).

Given that the vegetation index in the bare region varies widely and is affected by soil reflectance and biocrust, pixels with mean annual NDVI<sub>max</sub> less than 0.1 were masked (Smith et al., 2019). Besides, the water area was also eliminated.

## 3. Methods

### 3.1. Datasets and processing

Normalized Difference Vegetation Index (NDVI), is defined as  $(\text{NIR} - \text{RED}) / (\text{NIR} + \text{RED})$ , where NIR and RED are reflectance values in the near-infrared and red wavebands, respectively (Higginbottom and Symeonakis, 2014). NDVI represents the physiological activities of vegetation and it is the most used vegetation index as a measure of vegetation greenness and a proxy for ecosystem productivity (Smith et al., 2019). GIMMS NDVI dataset was produced from Advanced Very High Resolution Radiometer (AVHRR) instruments that extends from 1981 to the present with a semi-monthly temporal resolution and a  $1/12^\circ$  resolution. Calibration errors in the Global Inventory Monitoring and Modeling System Version 3 NDVI (GIMMSv3.0 g) dataset caused significant errors in the degradation detection over some of Australia's dryland regions. These errors have been addressed in the updated GIMMSv3.1 g which is strongly recommended by Burrell et al. (2018). GIMMSv3.1 g from 1982 to 2015 was obtained from the National Aeronautics and Space Agency (Pinzon and Tucker, 2014) and is available from the web page ("<https://ecocast.arc.nasa.gov/data/pub/gimms/>"). The dataset was resampled using the principle of first-order conservation remapping in ArcGIS10.5 from  $1/12^\circ$  to 0.1 to match the resolution of precipitation. The monthly NDVI was derived from the mean semi-monthly value and NDVI<sub>max</sub> is the largest value of the year.

The dataset of precipitation in Southern Africa is needed to calculate the response of vegetation to the dynamics of precipitation. The Multi-

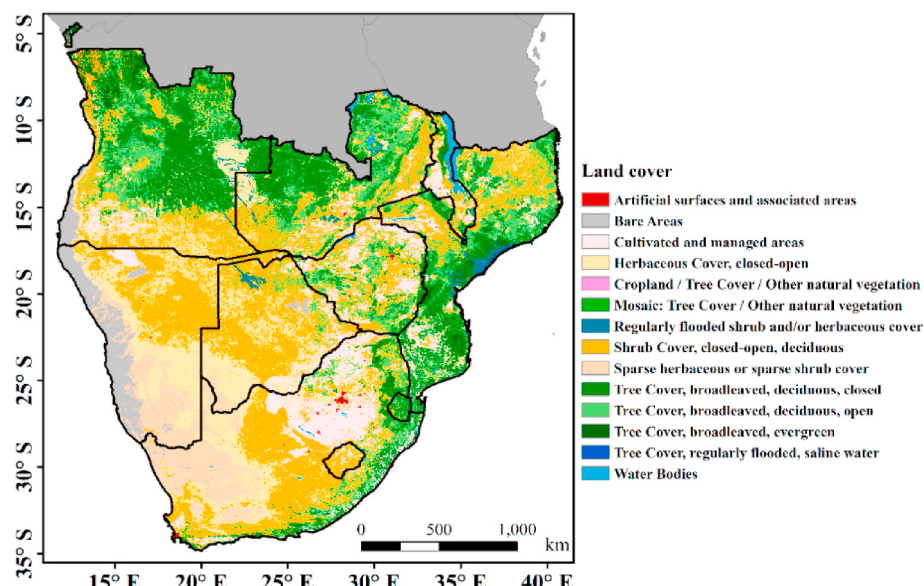


Fig. 1. The land cover in Southern Africa.

Source Weighted-Ensemble Precipitation version 2 (MSWEP V2) dataset is a novel fully global historic precipitation dataset (1979–2017) with a three-hourly temporal resolution and a  $0.1^\circ$  resolution derived by optimally merging a range of the gauge, satellite, and reanalysis estimates. According to the comparison with other datasets, MSWEP V2 performs better in long-term mean precipitation estimates for global, land, and ocean domains (Beck et al., 2019). The dataset of MSEWP is available from the website: "<http://www.globo2o.org/>". Given the effect of offset between the response of vegetation and the dynamics of precipitation, the period of precipitation needs to extend 2 years before NDVI. Therefore, MSWEP V2 from 1980 to 2015 was obtained to match the period of GIMMS3.1 from 1982 to 2015.

Global Land Cover 2000 (GLC, 2000) was produced with a 1-km spatial resolution with data from four sensors on-board Earth-observing satellites, each source of which was selected to map a specific ecosystem or land cover, seasonality or water regime (Mayaux et al., 2004). To incorporate the experience of local knowledge into the process of mapping, this project called GLC2000 was based on that team of regional experts mapped each continent independently. This makes sure that optimum image classification methods were used and that the land cover legend was regionally appropriate. In the first level, the classes include seven types: forests, woodlands and shrublands, grasslands, agricultural lands, bare soils, other land-cover classes, and the second level includes 27 classes. The land cover map of Africa used in this study can be requested from the Joint Research Centre, either through the Web pages of the Global Vegetation Monitoring Unit, (<https://www.gvm.jrc.it/glc2000/ProductGLC2000.htm>). According to the importance and the proportion of land cover, for degradation analyses of different land cover, the following land-cover classes were used: tree cover (including different tree cover in Fig. 1), shrub cover, herbaceous cover, sparse cover (sparse herbaceous and sparse shrubs), cultivated areas, bare areas, and artificial surfaces.

### 3.2. Linear regression

Linear regression is used to calculate the  $\text{NDVI}_{\max}$  trend which can be accomplished in R studio (February 1, 5033) with R package "lm" downloaded from "<https://cran.r-project.org/>". The following equation was used in this study:

$$y = a * x + b + \varepsilon$$

where  $y$  is annual  $\text{NDVI}_{\max}$ ;  $x$  is time (from 1982 to 2015);  $a$  is the slope or rate of change of  $\text{NDVI}_{\max}$ ;  $b$  is the intercept, and  $\varepsilon$  is an error. Linear regression was used to calculate the correlation between precipitation and  $\text{NDVI}_{\max}$  and the trend of the residuals over time in RESTREND analyses. The residual trend was taken as significant when  $p < 0.1$  and the VPR was taken as significant when  $P < 0.05$ .

### 3.3. RESTREND analysis

Residual trend (RESTREND) analysis was used to detect degradation without impact from precipitation, which can be accomplished in R studio (February 1, 5033) with R package "lm" downloaded from "<https://cran.r-project.org/>". To eliminate the influence of precipitation from NDVI, optimal accumulated precipitation was calculated on every pixel by finding which combination of accumulation period (1–12 months) and offset period (0–3 months) produced the highest and positive correlation coefficients ( $p < 0.05$ ) with annual  $\text{NDVI}_{\max}$  (Burrell et al., 2017). The next step was to calculate the vegetation-precipitation relationship (VPR) (Wessels et al., 2012). Then the residual trend (RESTREND) of VPR was calculated by regressing the VPR residuals to time (Wessels et al., 2012).

### 3.4. TSS-RESTREND analysis

#### 3.4.1. The procedures of TSS-RESTREND

Time Series Segment and Residual Trend (TSS-RESTREND) was used to detect degradation with breakpoints considered and with impact from precipitation eliminated, which can be accomplished in R studio (February 1, 5033) with R package "TSS.RESTREND" downloaded from "<https://cran.r-project.org/>". The procedures to calculate the time series of residual is the same as RESTREND mentioned in 3.3.

#### 3.4.2. Breaks for Additive Seasonal and Trend (BFAST) and the Chow test

BFAST was widely used to assess structural change, which divided time series into seasonal components and trend components (Bai and Perron, 2003). With the stochastic fluctuation included in the time series of NDVI, BFAST has limitations in detecting breakpoints with the low accuracy of detection. But considering the independence between residual and precipitation, detecting breakpoints with residuals can improve the accuracy of breakpoints detection. In TSS-RESTREND analysis, BFAST was applied to identify potential breakpoints with complete time-series residuals (Burrell et al., 2017). To avoid that segmented series were too short, 0.15 times (5 years) the whole study period (1982–2015) was set as the shortest allowable segment. The Chow test is used to test for equality between sets of coefficients in two linear regressions (Chow, 1960). The null hypothesis of a Chow test is that there is no change in the regression coefficients across a potential breakpoint. The null hypothesis is rejected if the  $F$ -statistic reaches the critical threshold ( $\alpha = 0.05$ ) (Burrell et al., 2017). In this study, the Chow test will test the significance of breakpoints in VPR and residual trend.

#### 3.4.3. Piecewise linear regression

Piecewise linear regression is calculated by the following equation:

$$Y_i = \beta_0 + \beta_1 X_i + \beta_2 Z_i + \beta_3 X_i Z_i$$

When a significant breakpoint was detected by BFAST and Chow test, piecewise regression was used to fit the residual trend and VPR before and after the breakpoint, where  $y$  is residual(or  $\text{NDVI}_{\max}$ ),  $x$  is years(or precipitation),  $z$  is the value of the dummy variable (0 or 1),  $\beta_0$  is the intercept,  $\beta_1$  is the slope,  $\beta_2$  is the offset at the breakpoint, and  $\beta_3$  is the change in slope at the breakpoint.

#### 3.4.4. Techniques used to determine results

According to whether the VPR and breakpoint are significant, the techniques used in the calculation can be divided into five categories (Fig. 4). *Indeterminate* refers to an insignificant relationship between precipitation and vegetation without significant breakpoint. *Agricultural regions* refers to a negative VPR. *RESTREND* refers to significant VPR, but without significant breakpoints in the residual change trend or in VPR, which is equal to the RESTREND method mentioned in 3.3. *VPR Change Detected* refers to the area where VPR and the residual trend have changed significantly during the study period. *Segmented RESTREND* indicates significant breakpoint only in residual. Among these types, only *VPR Change Detected* and *Segmented RESTREND* have breakpoints (Burrell et al., 2017).

#### 3.4.5. Total change and the direction of change

The total change was calculated by adding the significant VPR break height to the significant residual change (Burrell et al., 2017). The significance of VPR break height was tested by the  $t$ -test, and if  $p > 0.1$ , the VPR break height was taken as 0. The significance of residual change was tested by the  $F$ -test, and if  $p > 0.1$ , the residual change was taken as 0. The direction of the residual change was obtained by the predicted value in 2015 minus the predicted value in 1982. The significance of the change was the  $p$ -value of the  $F$ -test. D1 ( $p < 0.01$ ), D2 ( $0.01 < p < 0.025$ ), and D3 ( $0.025 < p < 0.05$ ) represent obvious decreases in vegetation productivity, whereas I1 ( $p < 0.01$ ), I2 ( $0.01 < p < 0.025$ ),

and I3 ( $0.025 < p < 0.05$ ) represent increasing productivity. DNC ( $0.05 < p < 0.1$ ) and INC ( $0.05 < p < 0.1$ ) represent observable decreasing and increasing trends respectively (Li et al., 2016). For comparison among these methods, the results of RESTREND (Fig. 5b) and linear trend analysis (Fig. 5c) were also calculated.

## 4. Results

### 4.1. Vegetation-precipitation relationship and breakpoints

#### 4.1.1. Vegetation-precipitation relationship

In southern Africa, aridity index declines from northeast to southwest (Zomer et al., 2008), and those pixels with vegetation growth controlled by the recent rainfall combination (Fig. 2b&d) (1–4 months' accumulated precipitation and 0 offsets) are mainly distributed in the southwestern portion of the study area (Fig. 2a&c). Besides, the pixels in the northern of study area are found without significant VPR (Fig. 2a&c). These spatial patterns demonstrate that the drier the environment, the stronger is the relationship between NDVI<sub>max</sub> and precipitation, which is similar to the results reported by Hellén et al. (2008) and Seddon et al. (2016).

#### 4.1.2. Breakpoints and techniques

Setting 5 years as the shortest segment, the timing of breakpoints ranged from 1986 to 2010 (Fig. 3b) and pixels with breakpoints made up 18.9% of the entire study area. Overall, the number of breakpoints increased from 1986 to 2010. The frequency of breakpoints in 1988, 1995, 1998, 1999, 2005, and 2010 is relatively higher than the adjacent years. The calibration periods of satellite sensors that are probably

detected as breakpoints are 1988, 1994, 2000, 2003, and 2008 (Burrell et al., 2017). However, besides 1988, no apparent agreement was found between frequency peaks and calibration periods. In space, breakpoints were mainly distributed along the western coast of Southern Africa, in which there were several spatial clusters with breakpoints in the same year, for example, a region in the western part of South Africa with breakpoints in 2009, a region along the west coast of South Africa and Namibia with breakpoints in 2006, and a region in the northern part of Namibia with breakpoints in 1998.

As Fig. 4 show, the most widely applicable method was RESTREND, which could be used in 54.4% of the study area. The pixels with RESTREND were mostly distributed in the southern part of the study area, including southern Zimbabwe, South Africa, Botswana, Namibia, and southern Mozambique. Pixels with *indeterminate* results made up 26.1% of the study area and were mostly distributed in Zambia, Angola, northern Zimbabwe, and northern Mozambique. Pixels with *Segmented RESTREND* and *VPR Change Detected* made up 6.9% and 12% of the study area respectively and were mainly distributed in the western part of the study area. Pixels classified as *Agricultural regions* made up only 0.7% of the study area. Pixels with significant breakpoints in VPR or residual trend made up 18.9% of the study area, which indicates that the assumptions of the TSS-RESTREND method are closer to the variability of VPR and residual dynamics than those of RESTREND.

### 4.2. Dynamics of vegetation detected by TSS-RESTREND, RESTREND, and linear trend analysis

Table 1 lists the specific percentages for the various results. “increasing” refers to a significant increase ( $p < 0.1$ ), “decreasing” refers

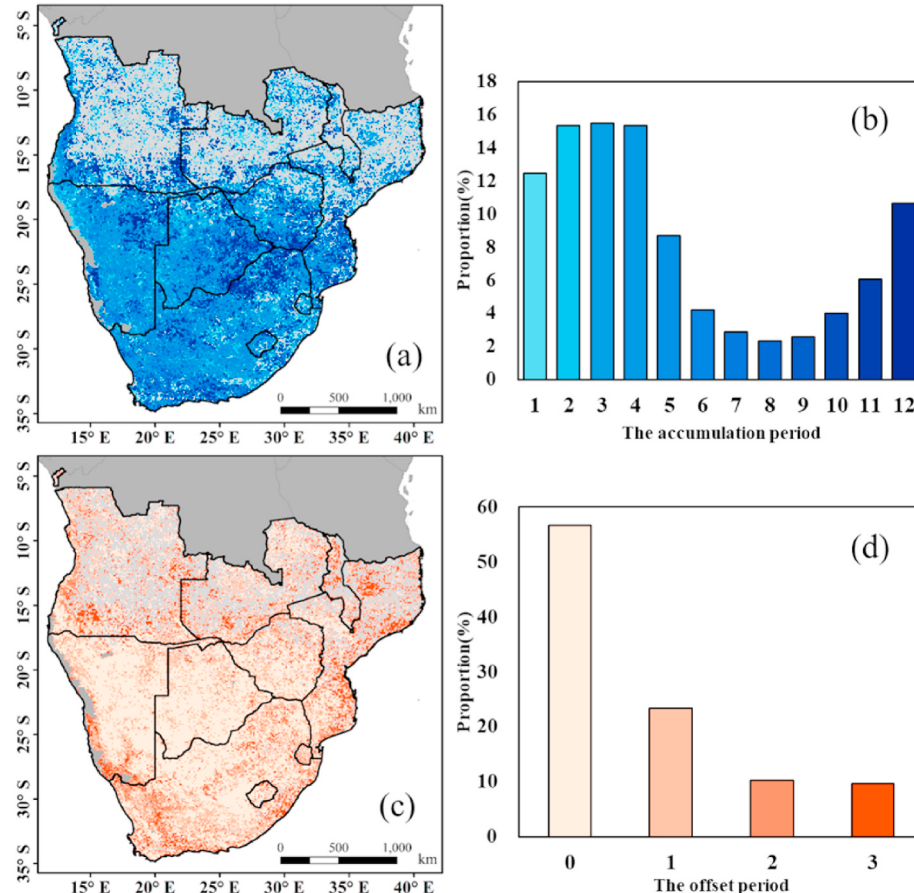


Fig. 2. Spatial patterns of (a) accumulation period and (c) offset period (pixels with insignificant VPR( $P > 0.05$ ) are in grey); proportion (%) for (b) the accumulation period and (d) the offset period.

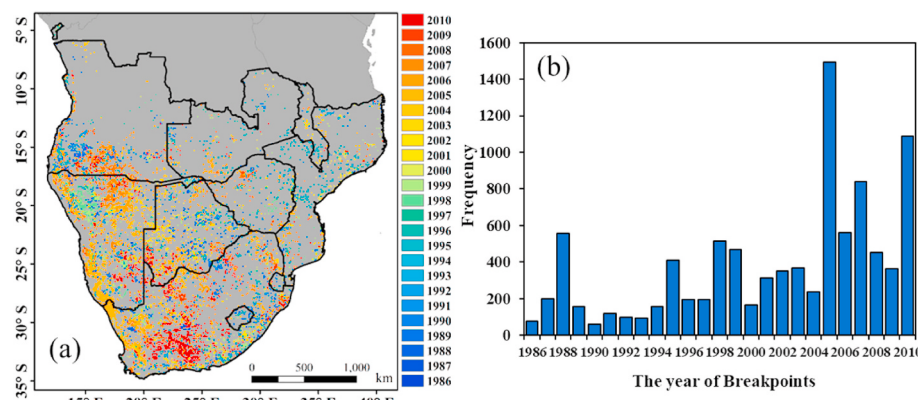


Fig. 3. (a) Spatial patterns and (b) frequency of significant breakpoints in VPR or residual.

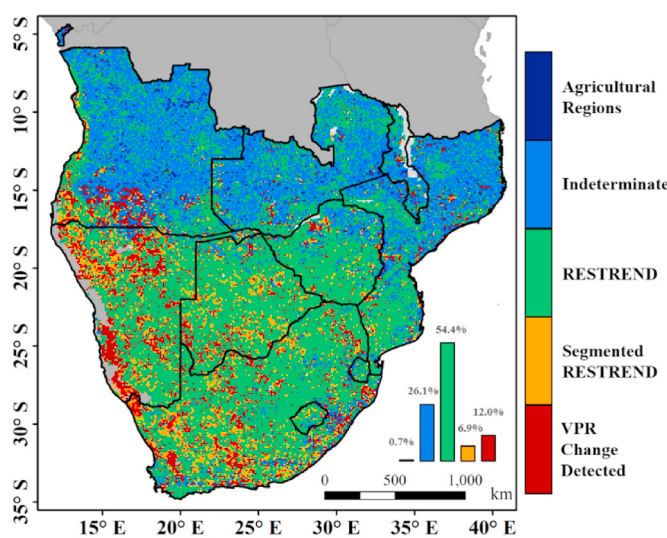


Fig. 4. Technique used to determine results. *Indeterminate* refers to an insignificant VPR without significant breakpoint. *Agricultural regions* refers to a negative VPR. *RESTREND* refers to significant VPR without significant breakpoints. *VPR Change Detected* refers to the area significant breakpoint in VPR. *Segmented RESTREND* indicates significant breakpoint only in residual.

to a significant decrease ( $p < 0.1$ ), “unchanged” refers to an insignificant increase or decrease ( $p > 0.1$ ), and “indeterminate” refers to an insignificant or negative relationship between annual NDVI<sub>max</sub> and precipitation; This class “indeterminate” includes pixels of *indeterminate* and *agricultural regions*. Using TSS-RESTREND, these increasing, decreasing, unchanged, and indeterminate pixels respectively made up 21.32%, 9.67%, 42.23%, and 26.78% of the study area; this result was different from those found by the other two methods. For example, more increasing trends were detected by linear trend analysis, and fewer decreasing trends were detected by RESTREND.

Fig. 5 shows the spatial pattern of the results obtained by RESTREND, linear trend analysis, and TSS-RESTREND. According to the results from TSS-RESTREND, the degraded areas were mainly located in western South Africa, the northwestern and southern Namibia, southwestern Angola, southern Mozambique, and southeastern Zimbabwe. The improved areas were concentrated to the southeast, center, and west of the study area, including eastern South Africa, eastern and southwestern Zimbabwe, eastern Namibia, and central and northern Botswana. Compared with linear trend analysis, more degradation was detected in the western part of South Africa, the northwestern and southern parts of Namibia, and southwestern Angola, and less improvement was observed in the southeastern portion of the study

area. However, in the northern part of the study area, TSS-RESTREND was not applicable due to the insignificant VPR. Compared with RESTREND, the TSS-RESTREND method found more land degradation in the southern part of Namibia and the western part of South Africa (Fig. 5b&c).

#### 4.3. Impacts of precipitation and breakpoints on the dynamics of vegetation

The difference between the total change obtained from TSS-RESTREND and RESTREND represents the effect of breakpoints (Fig. 6a). The effects of breakpoints were mainly negative in the western part of South Africa, the northern part of Namibia, and the southern part of Angola. The effect of precipitation on NDVI was obtained by subtracting the total change in TSS-RESTREND from the total annual change in NDVI<sub>max</sub> (Fig. 6b). As Fig. 6b shows that precipitation induced positive dynamics in most of the study area but had a slight negative effect in the northern part of Namibia and the southern part of South Africa. Fig. 7 shows in detail how the direction of change transformed from linear trend analysis and RESTREND to TSS-RESTREND. The highest percentages of transformed pixels between linear trend analysis and TSS-RESTREND were 16.92% of pixels from increasing to unchanged and 5.31% of pixels from unchanged to decreasing (Fig. 7a). The highest percentages of transformed pixels between RESTREND and TSS-RESTREND were 3.51% of pixels from increasing to unchanged and 3.76% of pixels from unchanged to decreasing (Fig. 7b).

## 5. Discussions

### 5.1. Relationship between precipitation and vegetation

For the entire study area, 73.21% of pixels demonstrated significant VPR, which indicates that in Southern Africa, vegetation growth is mainly controlled by rainfall, and highlights the need to use residual analysis to eliminate rainfall impacts on degradation detection. The growing season in southern hemisphere is from October to March. But in this study, we didn't include the whole growing season in the same year, which may influence the results to some extent. However, considering that the NDVI<sub>max</sub> may occur in a certain month and Dent et al. (2009) had proved that the influence of used calendar year made no difference on VPR, thus we think the impact will be small in this study.

Due to the introduction of new grain varieties and farming practices and increased irrigation, NDVI<sub>max</sub> continually increases, whereas precipitation decreases (Burrell et al., 2017). In this situation, these pixels with negative correlation between NDVI<sub>max</sub> and precipitation were classified as *Agricultural regions* by Burrell et al. (2017). Referring to GLC 2000 (Fig. 1), large areas of cultivated and managed areas are in the southern portion of Angola, the northern part of Namibia, the

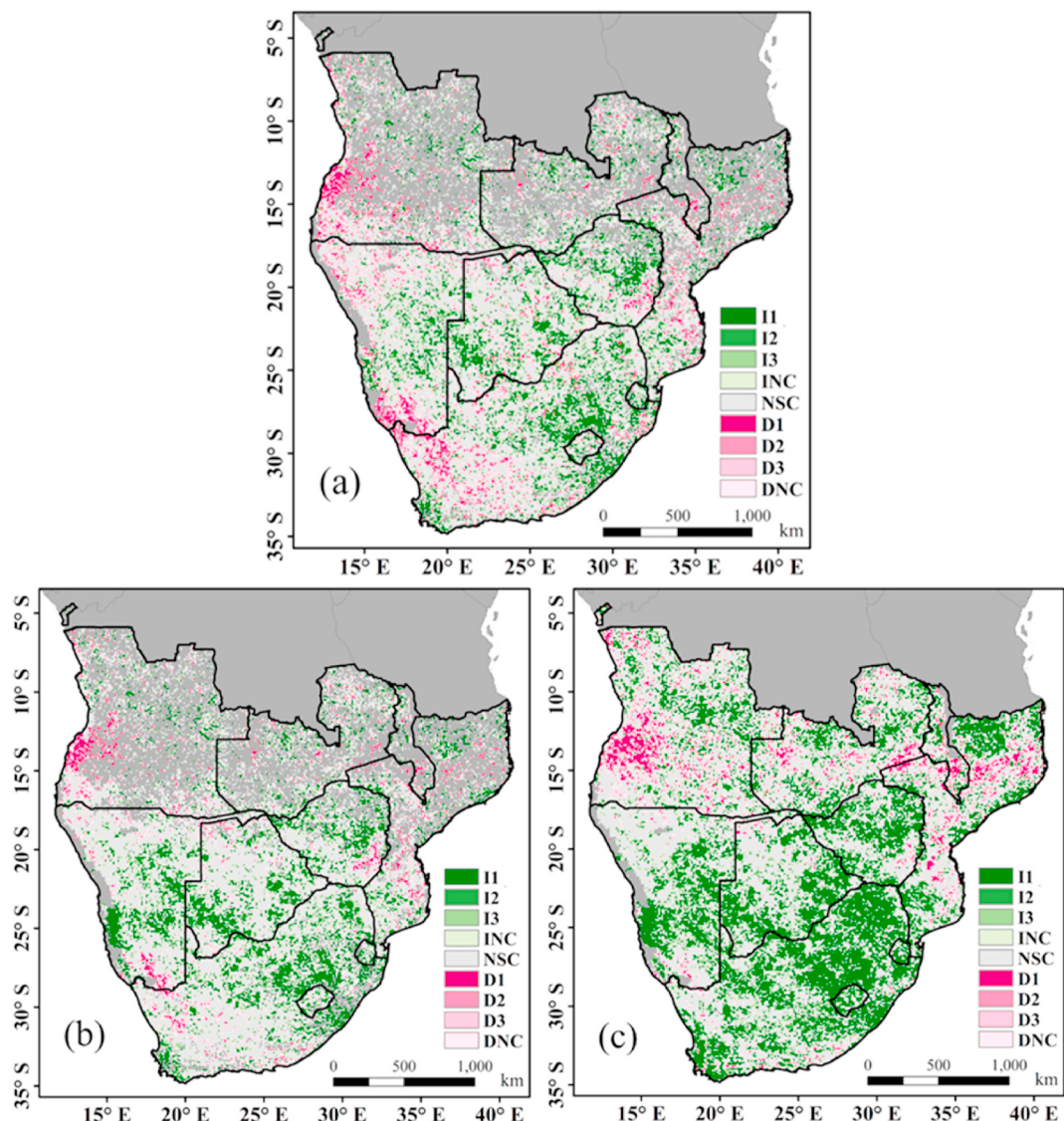


**Fig. 5.** The spatial pattern of the direction of change decreasing (red) and increasing (green) refer to land degradation and improvement respectively. The classification of the significance of change refers to 3.4.4; The direction of change detected by (a) TSS-RESTREND, (b) RESTREND and (c) linear trend analysis; Pixels in dark grey represent insignificant VPR. (For interpretation of the references to colour in this figure legend, the reader is referred to the Web version of this article.)

**Table 1**  
Percentages for the various results (%).

	Increasing	Decreasing	Unchanged	Indeterminate
Linearity	45.14	8.22	46.64	-
RESTREND	22.95	5.17	41.92	29.96
TSS-RESTREND	21.32	9.67	42.23	26.78

southwestern and eastern parts of South Africa, and Zimbabwe. However, these regions have been detected as showing significant VPR or breakpoints (Fig. 4), which indicates that the growth of these crops mainly relies on rainfall. Therefore, we think that the influence of irrigation is relatively low and will not alter the results of degradation detection much. Moreover, the criteria of detection for *Agricultural regions* is not suitable for the crops fed by precipitation in Southern Africa.

## 5.2. Implications and causes of breakpoints

Considering the presence of short-time disturbances, the breakpoint years in the beginning or at the end of the study period must be

interpreted carefully (Pan et al., 2018; Wessels et al., 2012). A pixel in the western part of South Africa with a residual breakpoint in 2010 was detected to have more reduction (red bar) than without a breakpoint (grey dotted line) (Fig. 8). Although the breakpoint induced by the fluctuation of high values in 2011, 2012, and 2013 may be misleading, it is hard to validate the cause of the disturbance. However, many pixels with breakpoints in 2010 and 2009 were identified (Fig. 3a), demonstrating the presence of a large-scale influence in these two years. Degradation with breakpoint in residual and VPR indicate the light degradation and the severe degradation respectively (Burrell et al., 2017) and in this study, two kinds of breakpoints mainly distributed in the transition area from bare cover to herbaceous cover to shrub cover (Figs. 1 and 4). Considering the perturbation from climate change, the ecosystem may shift from one to another alternative state (Hu et al., 2018), which will be detected as breakpoints in VPR or residual.

When considering breakpoints, the dynamics of ecosystem structure and trend lead to a more complex process. For example, with significant breakpoints, the degradation in southern Namibia and northern Angola were detected (Fig. 5a). However, residual trend in these areas have shifted from decline to incline (Fig. 9), which means the degradation

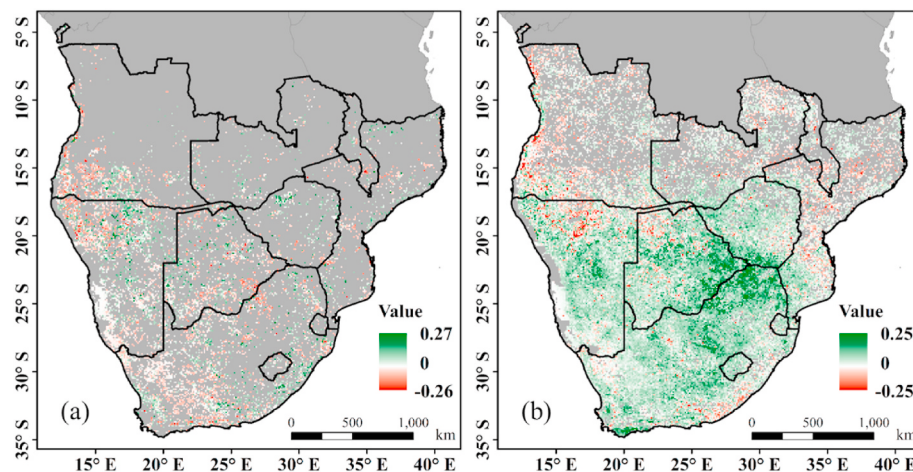


**Fig. 6.** (a) Impacts from breakpoints calculated with total change detected by TSS-RESTREND minus total change detected by RESTREND; (b) impacts from precipitation calculated with total change detected by Linearity minus total change detected by TSS-RESTREND.

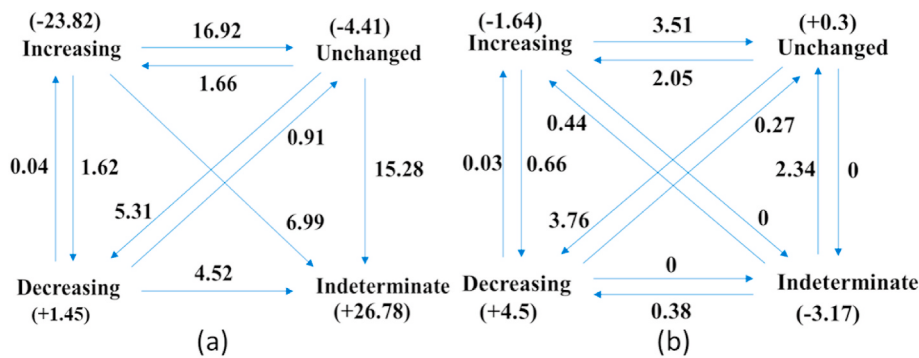


**Fig. 7.** Details in the transformed proportion of direction of change from (a) linear trend analysis and (b) RESTREND to TSS-RESTREND.

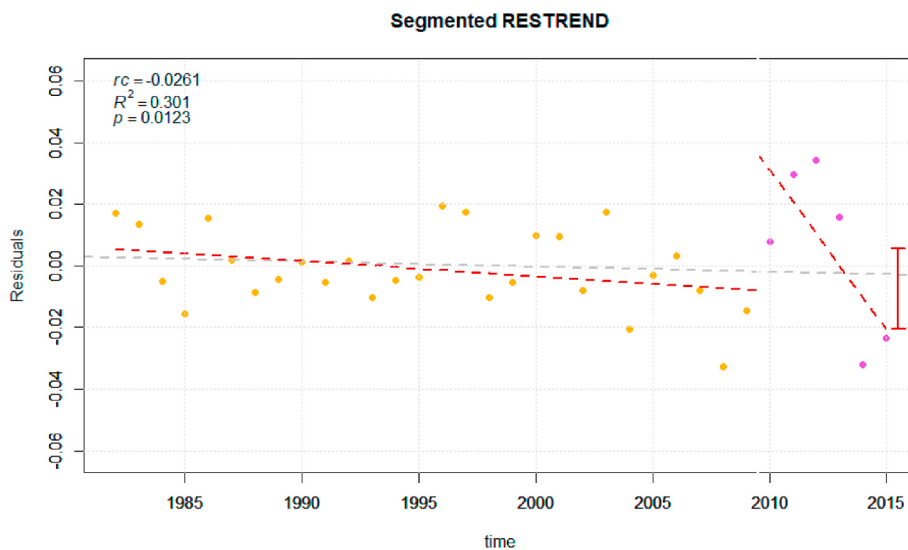


**Fig. 8.** Pixel in western South Africa with a breakpoint in 2010.

will be reversed in the long-term. To specify how land degradation happened and how to develop, further research will be needed to focus on breakpoints.

### 5.3. Possible factors inducing vegetation dynamics

The residual trend represents the part of NDVI not induced by precipitation dynamics. To specify the factors, the percentages of results in different land-cover classes were calculated (Fig. 10), and the results were verified with other literature published.

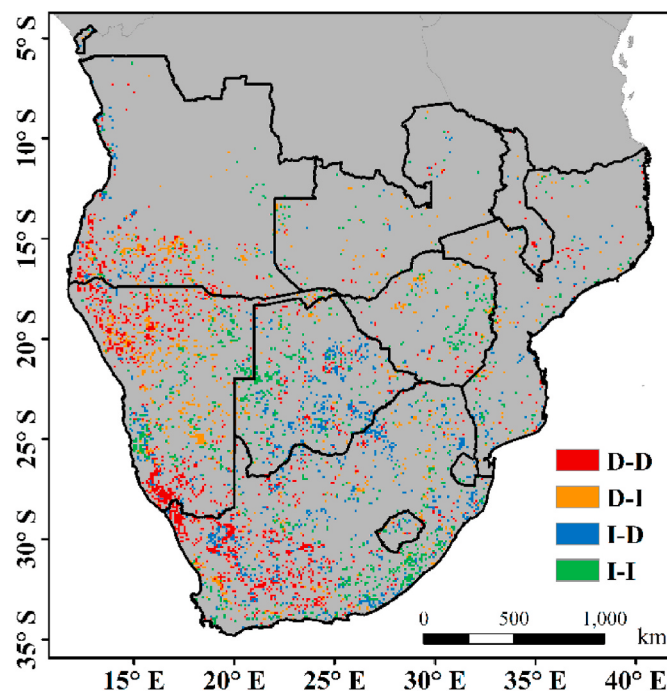


**Fig. 9.** Turning classification, D-D, transform from decreasing to decreasing; D-I, transform from decreasing to increasing; I-D, transform from increasing to decreasing; I-I, transform from increasing to increasing.

By field investigation, the Global Assessment of Human-Induced Soil Degradation (GLAOD) mapped the soil degradation pattern in 1991 (Oldeman, 1992). According to GLAOD, in the northwestern part of Namibia and the western part of South Africa, medium and very high water erosion severity exists. Besides, the erosion may also be intensified by the increasing precipitation. Therefore, the soil erosion is the potential explanation for the land degradation in the western part of South Africa, which is consistent with the relatively higher percentages of decrease in bare area and sparse cover (Figs. 1 and 10). In the northern part of Namibia, commonly owned areas were used intensively and tended to become more and more intensified (Unced, 2005). The pattern of the most intensely used areas is similar to the distribution of degradation in northern Namibia (Fig. 5a). This places the ecosystem in northern Namibia under a high risk of degradation (Klintenberg and Seely, 2004). Beside, by interpreting remote-sensing images, urbanization has also been related to reductions in ecosystem productivity in northern Namibia (Wingate et al., 2019). In sub-Saharan Africa, many charcoal-related industries have been increasing as agriculture expands and have destroyed forest and induced land degradation (Schneibei

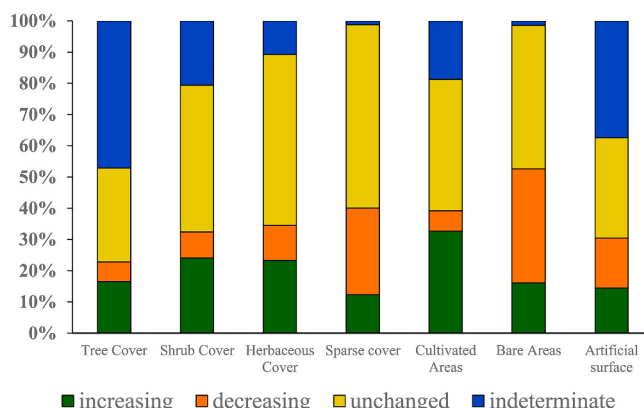


**Fig. 10.** Percentages of results in the different land-cover classes.

et al., 2017). Therefore, in this study, other degraded areas like western Angola and central Mozambique are probably related to the destroyed tree cover (Figs. 1 and 5a).

Saha et al. (2015) compared the distributions of shrub encroachment and improved area in southern Africa from 2001 to 2015 and proposed a relationship between them. The relatively higher percentage of increase in shrub and herbaceous cover has supported evidence of shrub encroachment (Fig. 10). Besides this, the increased CO<sub>2</sub> concentration has become the main factor in greening (Zhu et al., 2016), which can increase the use effectiveness of plants and mitigate pressure on water resources, especially in arid regions (Lu et al., 2016). Cultivated areas had the highest percentage of increasing (Figs. 5a and 10), which suggests that the effect of humans may increase the productivity of crop fields (Chen et al., 2019). A comparison with the FAO dataset demonstrates that in Southern Africa, the harvested area has continually declined from 1961 to 2017, but total production has steadily increased (FAOSTAT, 2019), which highlights the increasing productivity per unit of cropland.

#### 5.4. Degradation masked by the impacts of precipitation and breakpoints

The TSS-RESTREND method identified 4.5% degradation more than RESTREND (Fig. 7b), which may be induced by soil erosion and intensified land use. This shows that the TSS-RESTREND method has relative advantages over the RESTREND method in identifying degradation with breakpoints. Moreover, TSS-RESTREND found 23.82% of the study area with improvement less and 1.45% of the study area with degradation greater than that predicted by the linear trend method. However, TSS-RESTREND detects degradation with the residual trend, while the Linearity method detects degradation with time series of NDVI<sub>max</sub>, which are different two parts of vegetation dynamics. According to the definition of degradation, it is hard to judge which method is better. But through the qualitative comparison with other literature, results detected by TSS-RESTREND may indicate degradation induced by potential factors except precipitation, which has the function as warning signals of degradation.

Although TSS-RESTREND is not suitable for all Southern Africa, it can correct potential overestimates of improvement induced by precipitation (Fig. 6a). For those pixels that are not controlled by precipitation, the results detected by the linear trend model can serve as complementary results to those from TSS-RESTREND.

## 6. Conclusions

This study has applied the TSS-RESTREND method to detect land degradation masked by precipitation and breakpoints in southern Africa. For 73.22% of Southern Africa, vegetation growth is controlled by precipitation, and 18.9% of Southern Africa is affected by breakpoints, which indicates that TSS-RESTREND is useful for land degradation detection in Southern Africa. Also, TSS-RESTREND found that 21.32% of Southern Africa experienced positive change, 9.67% experienced negative change, and 42.23% had no significant change from 1982 to 2015. Compared with other literature, the potential explanations for degradation in the western part of South Africa degradation and in the northern part of Namibia are soil erosion and intensified use of commonly owned areas respectively. Through eliminating the positive effects from precipitation and including negative effects from breakpoints, TSS-RESTREND has highlighted the potential overestimates of improvement by the linear trend model and underestimates of degradation by the linear trend model and RESTREND. The results show that TSS-RESTREND can serve as a promising method for land degradation detection and the results of degradation detection with TSS-RESTREND are meaningful for land conservation and restoration. Finally, given the complex ecosystem dynamics at breakpoints, further research should be focused on how land degradation happens at breakpoints and how to develop after a breakpoint. As well, the ecological interpretations

behind residual need to be strengthened.

## Author contributions

S.W. designed the research. Z.L. conducted the research and wrote the first draft of the manuscript. S.W., S.S., Y.W., and W.M. reviewed and edited the manuscript. All the authors contributed to the discussion part.

## CRediT authorship contribution statement

**Zidong Li:** Writing - original draft, Writing - review & editing, conducted the research and wrote the first draft of the manuscript and made all the pictures. edited the manuscript and made the pictures and responded to reviewers. **Shuai Wang:** Writing - review & editing, designed the research. reviewed and edited the manuscript. made many valuable suggestions. **Shuang Song:** Writing - review & editing, reviewed and edited the manuscript. made many valuable suggestions. **Yaping Wang:** Writing - review & editing, reviewed and edited the manuscript. **Walter Musakwa:** Writing - review & editing, reviewed and edited the manuscript. All the authors contributed to the discussion part.

## Declaration of competing interest

The authors declare that they have no known competing financial interests or personal relationships that could have appeared to influence the work reported in this paper.

## Acknowledgments

This work was supported by the Strategic Priority Research Program of Chinese Academy of Sciences (XDA19030201), and the National Natural Science Foundation of China (No. 41761144064), and "the Fundamental Research Funds for the Central Universities".

## References

- Bai, J., Perron, P., 2003. Computation and analysis of multiple structural change models. *J. Appl. Econom.* <https://doi.org/10.1002/jae.659>.
- Bai, Z.G., Dent, D.L., Olsson, L., Schaeppman, M.E., 2008. Proxy global assessment of land degradation. *Soil Use Manag.* <https://doi.org/10.1111/j.1475-2743.2008.00169.x>.
- Beck, H.E., Wood, E.F., Pan, M., Fisher, C.K., Miralles, D.G., Van Dijk, A.I.J.M., McVicar, T.R., Adler, R.F., 2019. MSWep v2 Global 3-hourly 0.1° precipitation: methodology and quantitative assessment. *Bull. Am. Meteorol. Soc.* <https://doi.org/10.1175/BAMS-D-17-0138.1>.
- Burrell, A.L., Evans, J.P., 2018. ISPRS Journal of Photogrammetry and Remote Sensing the impact of dataset selection on land degradation assessment. *ISPRS J. Photogramm. Remote Sens.* 146, 22–37. <https://doi.org/10.1016/j.isprsjprs.2018.08.017>.
- Burrell, A.L., Evans, J.P., Liu, Y., 2017. Detecting dryland degradation using time series segmentation and residual trend analysis (TSS-RESTREND). *Remote Sens. Environ.* <https://doi.org/10.1016/j.rse.2017.05.018>.
- Cervigni, R., Morris, M., 2016. Confronting drought in Africa's drylands: opportunities for enhancing resilience. In: Confronting Drought in Africa's Drylands: Opportunities for Enhancing Resilience. <https://doi.org/10.1596/978-1-4648-0817-3>.
- Chen, C., Park, T., Wang, X., Piao, S., Xu, B., Chaturvedi, R.K., Fuchs, R., Brovkin, V., Ciais, P., Fensholt, R., Tømmervik, H., Bala, G., Zhu, Z., Nemani, R.R., Myneni, R.B., 2019. China and India lead in greening of the world through land-use management. *Nat. Sustain.* <https://doi.org/10.1038/s41893-019-0220-7>.
- Chow, G.C., 1960. Tests of equality between sets of coefficients in two linear regressions. *Econometrica*. <https://doi.org/10.2307/1910133>.
- Dent, D., Bai, Z., Schaeppman, M., Olsson, L., 2009. Letter to the editor - response to Wessels: comments on "Proxy global assessment of land degradation". *Soil Use Manag.* 25, 93–97. <https://doi.org/10.1111/j.1475-2743.2009.00197.x>.
- FAO, 2016. *Arid Zone Forestry: A Guide for Field Technicians*. FAO Corp. Doc. Repos.
- FAOSTAT, 2019. FAOSTAT: Statistical Database. FAOSTAT Stat. database [WWW Document].
- Hassan, R., 2005. Ecosystems and human well-being. *Current State and Trends 1. Current*.
- Helldén, U., Tottrup, C., 2008. Regional desertification: a global synthesis. *Global Planet. Change*. <https://doi.org/10.1016/j.gloplacha.2008.10.006>.
- Higginbottom, T.P., Symeonakis, E., 2014. Assessing land degradation and desertification using vegetation index data: current frameworks and future directions. *Rem. Sens.* <https://doi.org/10.3390/rs610952>.
- Hu, Z., Guo, Q., Li, S., Piao, S., Knapp, A.K., Ciais, P., Li, X., Yu, G., 2018. Shifts in the dynamics of productivity signal ecosystem state transitions at the biome-scale. *Ecol. Lett.* <https://doi.org/10.1111/ele.13126>.
- Kalisa, W., Igbawua, T., Henchiri, M., Ali, S., Zhang, S., Bai, Y., Zhang, J., 2019. Assessment of climate impact on vegetation dynamics over East Africa from 1982 to 2015. *Sci. Rep.* <https://doi.org/10.1038/s41598-019-53150-o>.
- Klinterberg, P., Seely, M., 2004. Land degradation monitoring in Namibia: a first approximation. *Environ. Monit. Assess.* <https://doi.org/10.1007/s10661-004-3994-6>.
- Li, X.B., Li, R.H., Li, G.Q., Wang, H., Li, Z.F., Li, X., Hou, X.Y., 2016. Human-induced vegetation degradation and response of soil nitrogen storage in typical steppes in Inner Mongolia, China. *J. Arid Environ.* <https://doi.org/10.1016/j.jaridenv.2015.07.013>.
- Lu, X., Wang, L., McCabe, M.F., 2016. Elevated CO<sub>2</sub> as a driver of global dryland greening. *Sci. Rep.* <https://doi.org/10.1038/srep20716>.
- Mathod, B., Kenabatho, P.K., Parida, B.P., Maphanyane, J.G., 2019. Evaluating land use and land cover change in the Gaborone dam catchment, Botswana, from 1984–2015 using GIS and remote sensing. *Sustain.* <https://doi.org/10.3390/su11195174>.
- Mayaux, P., Bartholomé, E., Fritz, S., Belward, A., 2004. A new land-cover map of Africa for the year 2000. *J. Biogeogr.* <https://doi.org/10.1111/j.1365-2699.2004.01073.x>.
- Oldeman, L.R., 1992. *Global Extent of Soil Degradation, Soil Resilience and Sustainable Land Use*.
- Pan, N., Feng, X., Fu, B., Wang, S., Ji, F., Pan, S., 2018. Increasing global vegetation browning hidden in overall vegetation greening: insights from time-varying trends. *Remote Sens. Environ.* <https://doi.org/10.1016/j.rse.2018.05.018>.
- Pinzon, J.E., Tucker, C.J., 2014. A non-stationary 1981–2012 AVHRR NDVI<sub>3g</sub> time series. *Rem. Sens.* 6, 6929–6960. <https://doi.org/10.3390/rs6086929>.
- Saha, M.V., Scanlon, T.M., Odorico, P.D., 2015. Examining the linkage between shrub encroachment and recent greening in water-limited southern Africa. *Ecosphere*. <https://doi.org/10.1890/ES15-00098.1>.
- Schneibl, A., Stellmes, M., Röder, A., Frantz, D., Kowalski, B., Haß, E., Hill, J., 2017. Assessment of spatio-temporal changes of smallholder cultivation patterns in the Angolan Miombo belt using segmentation of Landsat time series. *Remote Sens. Environ.* <https://doi.org/10.1016/j.rse.2017.04.012>.
- Sedano, F., Silva, J.A., Machoco, R., Meque, C.H., Sitoe, A., Ribeiro, N., Anderson, K., Ombe, Z.A., Baule, S.H., Tucker, C.J., 2016. The impact of charcoal production on forest degradation: a case study in Tete, Mozambique. *Environ. Res. Lett.* <https://doi.org/10.1088/1748-9326/11/9/094020>.
- Seddon, A.W.R., Macias-Fauria, M., Long, P.R., Benz, D., Willis, K.J., 2016. Sensitivity of global terrestrial ecosystems to climate variability. *Nature*. <https://doi.org/10.1038/nature16986>.
- Silva, J.A., Sedano, F., Flanagan, S., Ombe, Z.A., Machoco, R., Meque, C.H., Sitoe, A., Ribeiro, N., Anderson, K., Baule, S., Hurtt, G., 2019. Charcoal-related forest degradation dynamics in dry African woodlands: evidence from Mozambique. *Appl. Geogr.* <https://doi.org/10.1016/j.apgeog.2019.04.006>.
- Smith, W.K., Dannenberg, M.P., Yan, D., Herrmann, S., Barnes, M.L., Barron-Gafford, G. A., Biederman, J.A., Ferrenberg, S., Fox, A.M., Hudson, A., Knowles, J.F., MacBean, N., Moore, D.J.P., Nagler, P.L., Reed, S.C., Rutherford, W.A., Scott, R.L., Wang, X., Yang, J., 2019. Remote sensing of dryland ecosystem structure and function: progress, challenges, and opportunities. *Remote Sens. Environ.* <https://doi.org/10.1016/j.rse.2019.111401>.
- Spinoni, J., Vogt, J., Naumann, G., Carrao, H., Barbosa, P., 2015. Towards identifying areas at climatological risk of desertification using the Köppen-Geiger classification and FAO aridity index. *Int. J. Climatol.* <https://doi.org/10.1002/joc.4124>.
- Uncd, 2005. *Land Degradation Assessment in Drylands, Seventh Session of the Conference of the Parties item 10 of the provisional agenda*.
- UNCED, 1994. United Nations: convention to combat desertification in those countries experiencing serious drought and/or desertification, particularly in Africa. *Int. Leg. Mater.* <https://doi.org/10.1017/s0020782900026711>.
- Wei, F., Wang, S., Fu, B., Wang, L., Liu, Y.Y., Li, Y., 2019. African dryland ecosystem changes controlled by soil water. *Land Degrad. Dev.* <https://doi.org/10.1002/ldr.3342>.
- Wessels, K.J., Prince, S.D., Frost, P.E., Van Zyl, D., 2004. Assessing the effects of human-induced land degradation in the former homelands of northern South Africa with a 1 km AVHRR NDVI time-series. *Remote Sens. Environ.* <https://doi.org/10.1016/j.rse.2004.02.005>.
- Wessels, K.J., van den Bergh, F., Scholes, R.J., 2012. Limits to detectability of land degradation by trend analysis of vegetation index data. *Remote Sens. Environ.* <https://doi.org/10.1016/j.rse.2012.06.022>.
- Wingate, V.R., Phinn, S.R., Kuhn, N., 2019. Mapping precipitation-corrected NDVI trends across Namibia. *Total Environ.* <https://doi.org/10.1016/j.scitotenv.2019.05.158>.
- Xue, Y., Zhang, B., He, C., Shao, R., 2019. Detecting vegetation variations and main drivers over the agropastoral ecotone of northern China through the ensemble empirical mode decomposition method. *Rem. Sens.* <https://doi.org/10.3390/rs11161860>.
- Zhu, Z., Piao, S., Myneni, R.B., Huang, M., Zeng, Z., Canadell, J.G., Ciais, P., Sitch, S., Friedlingstein, P., Arneth, A., Cao, C., Cheng, L., Kato, E., Koven, C., Li, Y., Lian, X., Liu, Y., Liu, R., Mao, J., Pan, Y., Peng, S., Peuelas, J., Poultier, B., Pugh, T.A.M., Stocker, B.D., Viovy, N., Wang, X., Wang, Y., Xiao, Z., Yang, H., Zaehle, S., Zeng, N., 2016. Greening of the Earth and its drivers. *Nat. Clim. Change*. <https://doi.org/10.1038/nclimate3004>.
- Zomer, R.J., Trabucco, A., Bossio, D.A., Verchot, L.V., 2008. Climate change mitigation: a spatial analysis of global land suitability for clean development mechanism afforestation and reforestation. *Agric. Ecosyst. Environ.* <https://doi.org/10.1016/j.agee.2008.01.014>.